



저작자표시-비영리-변경금지 2.0 대한민국

이용자는 아래의 조건을 따르는 경우에 한하여 자유롭게

- 이 저작물을 복제, 배포, 전송, 전시, 공연 및 방송할 수 있습니다.

다음과 같은 조건을 따라야 합니다:



저작자표시. 귀하는 원저작자를 표시하여야 합니다.



비영리. 귀하는 이 저작물을 영리 목적으로 이용할 수 없습니다.



변경금지. 귀하는 이 저작물을 개작, 변형 또는 가공할 수 없습니다.

- 귀하는, 이 저작물의 재이용이나 배포의 경우, 이 저작물에 적용된 이용허락조건을 명확하게 나타내어야 합니다.
- 저작권자로부터 별도의 허가를 받으면 이러한 조건들은 적용되지 않습니다.

저작권법에 따른 이용자의 권리는 위의 내용에 의하여 영향을 받지 않습니다.

이것은 [이용허락규약\(Legal Code\)](#)을 이해하기 쉽게 요약한 것입니다.

[Disclaimer](#)

Combined therapy of focused ultrasound  
and aducanumab induces neurogenesis  
and decreases of beta-amyloid plaques in  
a mouse model of Alzheimer's disease

Chanho Kong

Department of Medicine

The Graduate School, Yonsei University

Combined therapy of focused ultrasound  
and aducanumab induces neurogenesis  
and decreases of beta-amyloid plaques in  
a mouse model of Alzheimer's disease

Directed by Professor Jin Woo Chang

The Doctoral Dissertation  
submitted to the Department of Medicine,  
the Graduate School of Yonsei University  
in partial fulfillment of the requirements for the degree of  
Doctor of Philosophy

Chanho Kong

December 2021

This certifies that the Doctoral Dissertation  
of Chanho Kong is approved.

---

Thesis Supervisor: Jin Woo Chang

---

Thesis Committee Member#1: Bae Hwan Lee

---

Thesis Committee Member#2: Jinna Kim

---

Thesis Committee Member#3: Se Hoon Kim

---

Thesis Committee Member#4: Chang Kyu Park

The Graduate School  
Yonsei University

December 2021

## ACKNOWLEDGEMENTS

I would like to express my gratitude to those who have supported me in completing my degree program and getting to where I am today.

First of all, I would like to express my sincere gratitude to my advisor, Professor Jin Woo Chang, for teaching and guiding me throughout the doctoral program. Professor Jin Woo Chang's attitude and passion for research ranging from basic science to clinical research will be a great foundation for my life. And also, I truly appreciate to Dr. Bae Hwan Lee, Dr. Jinna Kim, Dr. Se Hoon Kim and Dr. Chang Kyu Park for their academic advice and thoughtful comments on my dissertation.

I also would like to express my gratitude to Dr. Won Seok Chang, Dr. Hyun Ho Jung, and Dr. Young Cheol Na, who have helped me grow up as a researcher through various studies. And also, I would like to express my gratitude to the members of the stereotaxic neurosurgery family who have spent together for 7 years. In particular, I would like to thank Dr. So Hee Park.

During the course of my degree, I was able to learn various studies through many collaborative research. I would like to express my gratitude to the members of Prof. Sang Won Seo's laboratory at Hallym Univ., Prof. Hye Sun Kim's Lab at Seoul National Univ., and Prof. Sang Beom Jun's Lab at Ewha Womans Univ. In particular, I would like to thank Dr. Bo Young Choi.

Deeply thanks you to our lab members who studied together day and night. I would like to thank Dr. Chin Su Koh who helped me figure out answers

when I'm lost and cared me all the time. I would like to thank Dr. Bong Soo Kim for giving me valuable advice during my degree course. I would like to express my gratitude to Dr. Jaewoo Shin and Dr. Jihyeon Lee for teaching me many experiment skills, and to Jae Sung Cho and Min Sik Yoon who spent hard time together. I would like to express my deepest gratitude to Younghee Seo, Ji Young Park, Jiwon Beak, Sangheon Han, Tae Jun Kim, and Heesue Chang, and also special thanks to Junwon Park who are currently helping several research projects together. In particular, I would like to express my sincere gratitude to Minkyung Park, who has always been my supporter on my side encouraging me and gave joyful lab experiences.

I am extremely thankful to my friends, Dong Hee Kim, Nak Kyung Kim, Hoon Kim, Chang Yeop Baek, Yong Hoi Ahn, Chan Jin Yoo, Han Jin Yoo, Sang Woo Lee, Jong Wan Lee, Jae Min Jeong, Ju Yeol Jeong for their always valuable support.

Lastly, I would like to express my gratitude to my father, mother, Hyun Ji Kong, Hyun Gyu Shin and Mr. Keun Hong Kim, Mrs. Ju Young Koo who have always supported and prayed for me from afar, and I would like to thank God for allowing me to finish my doctorate.

With invaluable support from many people, I was able to finish my degree course. In the future, I will do my best to become a humble and passionate researcher in neuroscience.

December 2021

Chanho Kong

## <TABLE OF CONTENTS>

**ABSTRACT** ..... 1

**I. INTRODUCTION** ..... 4

**II. MATERIALS AND METHODS** ..... 7

**Part 1. Safety and efficiency of FUS in a 5xFAD mouse model of AD**

1. Animals ..... 7

2. Focused ultrasound system ..... 9

3. Blood–brain barrier opening and safety ..... 10

4. Focused ultrasound treatment ..... 11

5. Behavioral test: Morris water maze ..... 13

**Part 2. The combined therapy of FUS and aducanumab for AD**

1. Animals ..... 14

2. Drug: aducanumab ..... 14

3. Combined therapy of FUS and aducanumab ..... 15

4. Magnetic Resonance Imaging ..... 16

5. Behavioral test: spontaneous alteration in the Y-maze ..... 18

6. BrdU labeling ..... 18

7. Immunohistochemistry ..... 19

8. Statistical analysis ..... 20

<b>III. RESULTS</b> .....	21
<b>Part 1. Safety and efficiency of FUS in a 5xFAD mouse model of AD</b>	
1. Examination of safety for FUS – mediated BBB opening .....	21
2. FUS-induced BBB opening decreased amyloid plaques in the hippocampus .....	22
3. FUS-induced BBB opening improved the cognitive function in 5xFAD .....	24
<b>Part 2. The combined therapy of FUS and aducanumab for AD</b>	
4. Combined therapy of FUS and aducanumab rescued the cognitive impairments in 5xFAD .....	26
5. The combined therapy of FUS and aducanumab decreased amyloid plaques in the dentate gyrus of the hippocampus .....	28
6. The combined therapy of FUS and aducanumab increased neurogenesis in 5xFAD mouse .....	31
<b>IV. DISCUSSION</b> .....	35
<b>V. CONCLUSION</b> .....	41
<b>REFERENCES</b> .....	42
<b>ABSTRACT (in Korean)</b> .....	45
<b>PUBLICATION LIST</b> .....	48



## LIST OF FIGURES

- Figure 1.** Photograph of the PCR gene product for APP and PS1 in 5xFAD mice .....8
- Figure 2.** Scheme of the FUS system setup for BBB opening in mice .....9
- Figure 3.** Scheme of the experimental procedure ..... 12
- Figure 4.** Experimental timeline for combined therapy of FUS and aducanumab ..... 15
- Figure 5.** Confirmation of the FUS mediated BBB opening .. 17
- Figure 6.** Confirmation of BBB opening and evaluation of tissue damage .....21
- Figure 7.** FUS-mediated BBBO reduces A $\beta$  plaques .....23
- Figure 8.** FUS improves cognitive function and spatial memory .....25
- Figure 9.** The combined therapy of FUS and aducanumab restored cognitive impairments .....27
- Figure 10.** The combined therapy of FUS and aducanumab decreased A $\beta$  accumulation in 5xFAD mice .....29

<b>Figure 11.</b> Analysis of cell proliferation and neurogenesis in the DG of the hippocampus .....	33
<b>Figure 12.</b> Dose dependent aducanumab expression level delivered by FUS .....	38

## LIST OF TABLES

<b>Table 1.</b> Primer sequences .....	8
<b>Table 2.</b> MRI sequences and parameters .....	17

## ABSTRACT

### **Combined therapy of focused ultrasound and aducanumab induces neurogenesis and decreases of beta-amyloid plaques in a mouse model of Alzheimer's disease**

Chanho Kong

*Department of Medicine  
The Graduate School, Yonsei University*

(Directed by Professor Jin Woo Chang)

Focused ultrasound (FUS) with microbubbles (MBs) can noninvasively open the blood–brain barrier (BBB) for drug delivery into the parenchyma. In preclinical studies, it is known that FUS-induced BBB opening not only enhances the penetration of therapeutic agents but also modulates neurogenesis and immunity. Recently, human clinical trials in Alzheimer's disease (AD) with FUS treatment have been initiated. Beta-amyloid (A $\beta$ ) deposition is a typical pathological phenomenon of AD. Although its mechanism remains questionable and controversial as a target for AD treatment strategies, numerous studies have focused on targeting A $\beta$ . Meanwhile, numerous studies have reported that FUS-mediated BBB opening reduces A $\beta$  levels in the brain. As previously used drugs for AD are limited to relieve symptoms, studies are more inclined to develop drugs, and there is a trend to develop drugs that can solve the cause of the disease. Aducanumab is a human monoclonal antibody that

reduces A $\beta$  plaques in a dose-dependent manner. First, establishing FUS parameters to avoid blood vessel damage is an essential step to address safety issues and needs to be effective enough to open the BBB as well. Thus, the safety and efficacy of FUS-mediated BBB opening in the 5xFAD AD mouse model were examined, and whether FUS-mediated BBB opening contributes to the reduction of A $\beta$  and improved cognitive function was investigated. As a result, a safe and efficient parameter of FUS was developed (1-Hz burst repetition frequency, 10-ms bursts, 120s in total, and average peak pressure 0.25 MPa). It did not only cause any hemorrhages or damage in the brain, but also proved its effectiveness. FUS-mediated BBB opening decreased A $\beta$  in the hippocampus of 5xFAD mice and rescued cognitive function. Second, it was hypothesized that the combined therapy of FUS and aducanumab would be more effective than either FUS or aducanumab treatment alone. The effectiveness could be maximized depending on the number of treatments; FUS was targeted at four regions of the hippocampus where newly generated neurons occur, and aducanumab treatment was conducted three times biweekly and dose dependent. Combined therapy increased both proliferation and neurogenesis in the hippocampus. In line with this result, it was shown that the combined therapy significantly decreased A $\beta$  plaques in the hippocampus and restored cognitive function. In addition, its effectiveness was more statistically significant when treated multiple times. In conclusion, the combined therapy of FUS and aducanumab for AD reduced amyloid aggregation, restored spatial memory, and increased neurogenesis. Furthermore, the remarkable aspect of this study is that the combined therapy was shown to be effective even with the minimal dose of the drug by increasing the BBB penetration rate with FUS, while excluding the possibility of side effects. This study provides a better insight into establishing a solid therapeutic strategy for the treatment of AD as well

as other neurodegenerative diseases.

---

Key words: Alzheimer's disease, focused ultrasound, blood–brain barrier, beta-amyloid, aducanumab

**Combined therapy of focused ultrasound and aducanumab induces neurogenesis and decreases of beta-amyloid plaques in a mouse model of Alzheimer's disease**

Chanho Kong

*Department of Medicine  
The Graduate School, Yonsei University*

(Directed by Professor Jin Woo Chang)

## **I. INTRODUCTION**

Alzheimer's disease (AD) is the most common neurodegenerative disease that progressively deteriorates cognitive functions, including memory. Similar to other neurodegenerative diseases, as the pathogenesis is complex and affected by various factors, its underlying mechanism has not been elucidated clearly. Pathological features of AD include extracellular beta-amyloid (A $\beta$ ) plaques and intracellular neurofibrillary tangles, leading to neurodegeneration and cell death. Because A $\beta$  deposition contributes to the initiation of AD pathogenesis, therapeutic strategies that reduce or eliminate the production of A $\beta$  plaques have long been the basis for AD treatment.

However, a fundamental treatment method for the treatment of AD has not yet been developed. Instead, in clinical studies, the current first-line treatment for AD is administration of drugs, such as donepezil and galantamine, which alleviate symptoms and delay progression.<sup>1</sup> According to the recently reported Alzheimer's

drug development pipeline, recent treatment development tends to progress toward the fundamental treatment of the disease rather than merely focusing on symptom relief. It also suggests that amyloid-related therapeutics account for the largest proportion of the current pipeline of agents.<sup>2,3</sup> Although the correlation between A $\beta$  decrease and recovery in cognitive function is not well understood, reducing A $\beta$  aggregates associated with the onset of AD would be a promising target to establish a solid therapeutic strategy for AD.<sup>2,4-7</sup>

Aducanumab is a medication designed to treat AD and an A $\beta$ -directed human monoclonal antibody that selectively binds to the A $\beta$  protein. In a clinical trial of aducanumab in patients with a clinical diagnosis of prodromal or mild AD, A $\beta$  was decreased dose (3–10 mg/kg) dependently.<sup>8</sup> Consistent with the aforementioned outcome of clinical trials, an animal study using transgenic mice (Tg2576) showed that A $\beta$  was significantly reduced in the group administered with a dose of 10 mg/kg or higher.<sup>8</sup> Aducanumab has been approved for the treatment of AD and AD-derived mild cognitive impairment in the United States Food and Drug Administration in June 2021. It is the first new drug treatment for dementia to reach the United States market in almost 20 years. However, the approval is still controversial due to ambiguous clinical trial results regarding its efficacy.<sup>9,10</sup> Aducanumab is currently the most promising drug for the treatment of AD, as research results have reported reducing A $\beta$  even though its efficacy has not been fully demonstrated due to vague clinical trial results.<sup>8</sup>

The blood–brain barrier (BBB) is a unique structure that tightly regulates the transport of cells and molecules to restrict the penetration of noxious substances from the blood into the brain. Therefore, its permeability is highly selective to ensure optimal condition to maintain homeostasis of the central nervous system.<sup>11</sup> However,



its function has long been a challenge when potentially effective therapeutic agents are applied, as the BBB prevents about 98% of drug compounds from penetrating into the parenchyma.<sup>12</sup> Focused ultrasound (FUS) with microbubbles (MBs) is a minimally invasive or noninvasive approach for reversible and safe BBB opening.<sup>13</sup> Concentrating the acoustic pressure on the target area in the brain causes the cavitation effect of circulating MBs and temporarily opens the BBB.<sup>14</sup> As FUS is developed, research on drug delivery with FUS has been steadily progressing through the delivery of various therapeutic agents, such as chemotherapeutics,<sup>15-17</sup> cells,<sup>18,19</sup> and antibodies.<sup>20</sup> Furthermore, multiple evidence have reported that A $\beta$  decreased by only opening the BBB without delivering therapeutic agents in the AD mouse model.<sup>21</sup> In line with previous research, it has been also proposed that BBB opening by FUS induced adult hippocampal neurogenesis in rodents, implying that FUS has a potential to be an effective therapeutic strategy for AD.<sup>22,23</sup>

However, to date, whether aducanumab with FUS would be more effective than applying a drug alone and to what extent FUS can modulate A $\beta$  plaques and enhance cognitive functions remain unclear. To address these questions, this study aimed to demonstrate the effects of FUS, aducanumab, and the combined therapy of FUS and aducanumab in a 5xFAD AD mouse model in terms of A $\beta$  reduction, neurogenesis, and cognitive function.

## II. MATERIALS AND METHODS

### Part 1. Safety and efficiency of FUS in a 5xFAD mouse model of AD

#### 1. Animals

The 5xFAD mouse is a transgenic mouse with five familial mutations. These mice express high levels of both mutant human amyloid precursor protein (APP695) with Swedish mutation (K670N, M671L), London mutation (V717I), Florida mutation (I716V), and human presenilin 1 (PS1) with two mutations (M146L and L286V). 5xFAD mice were purchased from Jackson Laboratory (Sacramento, CA, USA) and maintained by crossing hemizygous transgenic mice with B6SJL F1 mice. Transgenic mice were identified by polymerase chain reaction (PCR), and non-transgenic littermates served as controls. Offspring were genotyped by PCR amplification using the APP and PSEN1 alleles (Table 1). The PCR products were separated on a 1% agarose gel. The APP and PSEN1 allele products were 377 bp and 608 bp, respectively (Figure 1). Extracellular amyloid deposition and gliosis beginning around 2 months are the main characteristics of 5xFAD.<sup>24</sup> Moreover, its phenotype can be defined as spontaneous alternation in the Y maze in that the impairment in spatial working memory begins at approximately 4 to 5 months of age.<sup>25</sup> Neuron loss has been observed in multiple brain regions in this model and begins at approximately 6 months of age.<sup>24,26</sup> All mice were housed in groups of 1–2 per cage with ad libitum access to food and water, in a humidity- and temperature-controlled, specific pathogen-free environment (12-h light cycle; lights on at 8 am) at the Yonsei University College of Medicine Animal Care Facility accredited by the Association for Assessment and Accreditation of Laboratory Animal Care. All

experimental procedures in this study were approved by the Institutional Animal Care and Use Committee of the Yonsei University Health System, Republic of Korea (IACUC no.: 2019-0213).

**Table 1. Primer sequences**

Gene	Forward sequence (5' – 3')
APP	AGG ACT GAC CAC TCG ACC AG
PSEN1	AAT AGA GAA CGG CAG GAG CA
GAPDH	AAT AGA GAA CGG CAC GAG CA
Gene	Reverse sequence (3' – 5')
APP	CGG GGG TCT AGT TCT GCA T
PSEN1	GCC ATG AGG GCA CTA ATC AT
GAPDH	GCC ATG AGG AGCA CTA ATC AT



**Figure 1. Photograph of the PCR gene products for APP and PS1 in 5xFAD mice.** Mutations in the genes for amyloid precursor protein (APP) and presenilins (PS1, PS2) increased the production of  $\beta$ -amyloid 42 ( $A\beta$ 42) and caused familial Alzheimer's disease.

## 2. Focused ultrasound system

A 0.5-MHz single-element focused transducer (H-107MR; Sonic Concepts, Bothell, WA, USA) was used, with a transducer diameter of 51.7 mm and a radius of curvature of 63.2 mm. The transducer was used with a conical container that could be filled with degassed water to efficiently transfer the acoustic energy. A waveform generator (33220A, Agilent, Palo Alto, CA, USA) was connected to a 40-dB radio frequency power amplifier (210 L, ENI Inc., Rochester, NY, USA) to drive the FUS transducer, and a power meter (E4419B, Agilent) was used to measure the input electrical power (Figure 2).

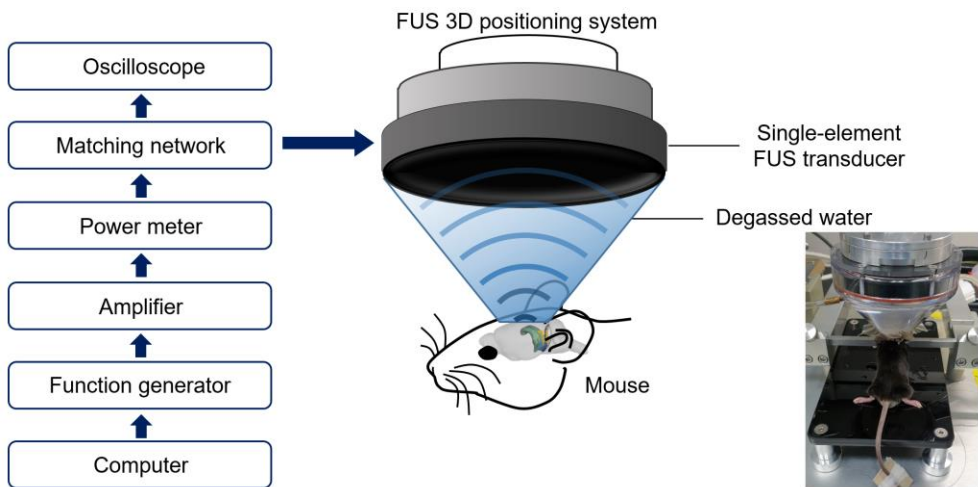


**Figure 2. Scheme of the FUS system setup for BBB opening in mice.**

### **3. Blood–brain barrier opening and safety**

To determine the FUS-mediated BBB opening efficiency and safety according to changes in sonication acoustic pressure amplitude, both Evans blue (EB) and histological tissue damage were confirmed in response to 0.22-, 0.23-, 0.24-, and 0.25-MPa acoustic pressures. EB, an albumin marker used to measure BBB permeability, was intravenously injected (2%, 100 mg/kg) immediately after FUS sonication. Hematoxylin and eosin (H&E) staining was performed to confirm brain damage.

#### 4. Focused ultrasound treatment

To confirm the changes in A $\beta$  followed by FUS treatment, sonication was performed on the hippocampus unilaterally (coordinates from bregma: AP - 2.0, ML + 1.2 mm) of 5xFAD (n = 3), and animals were sacrificed a week later (Figure 3A). To confirm the cognitive improvement of 5xFAD by FUS treatment, 6-month-old male 5xFAD mice were divided into four groups: sham (n = 13), sham + FUS (n = 11), TG (n = 7), and TG + FUS (n = 7) groups. During surgery, mice were anesthetized with 5% isoflurane in oxygen, and animal heads were fixed on a stereotaxic frame (Narishige, Tokyo, Japan). A medical sterile ultrasound gel (ProGel; Dayo Medical Co., Seoul, South Korea) was used to fill the space between a coupling cone filled with degassed water and the skull for energy transfer efficiency. The FUS was targeted to four focal spots (coordinates from bregma: AP - 1.6, ML  $\pm$  1.2 mm/AP - 2.6, ML  $\pm$  2.4 mm) on the hippocampus bilaterally (Figure 3B). DEFINITY MBs (0.04 mL/kg; Lantheus Medical Imaging, North Billerica, MA, USA) were injected intravenously after confirming the coordinates of the target point on the skull, and sonication (1-Hz pulse repetition frequency (PRF), 10-ms bursts, 120 s in total, and average peak pressure 0.25 MPa) was started at the same time (Figure 3C).

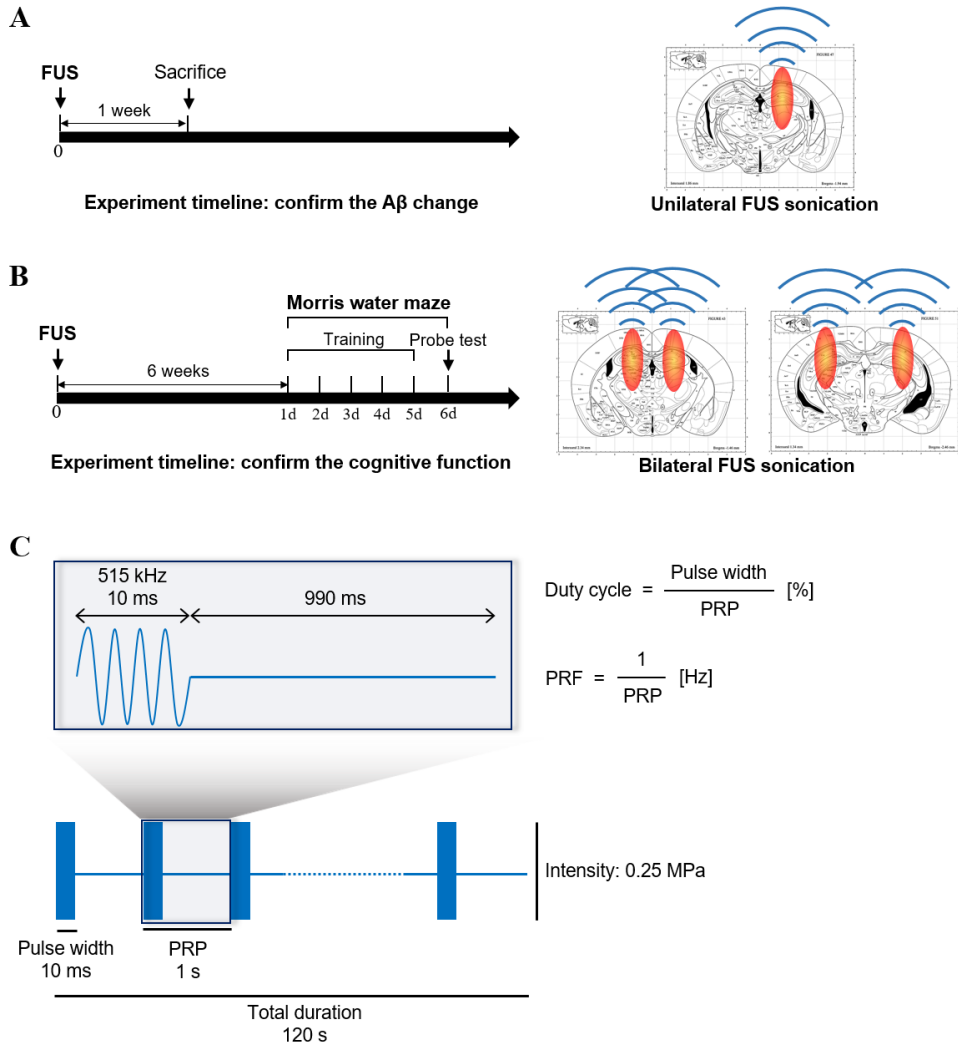


**Figure 3. Scheme of the experimental procedure.**

(A) To confirm the changes in A $\beta$ , the animals were sacrificed 1 week after sonication. FUS was sonicated unilaterally, and the contralateral brain was used as a control. (B) To confirm the cognitive function, sonication was performed on four spots of the hippocampus, and the Morris water maze test was performed 6 weeks after sonication. (C) The sonication parameters included an amplitude of 0.25 MPa, PRF of 1 Hz, pulse repetitive period (PRP) of 1 s, duty cycle of 1 %, and total sonication time of 2 min.

## 5. Behavioral test: Morris water maze

A water maze test was performed 6 weeks after FUS treatment to verify the improvement in cognitive function by FUS. A circular water pool (12 cm in diameter) was filled with water ( $23 \pm 2^\circ\text{C}$  temperature), and the water was mixed with edible dye (Bright White Liqua-Gel; Chefmaster, CA, USA) to make the water opaque, so the platform (10 cm in diameter) was not visible. Different-shaped visual cues were marked on the walls of the four quadrants: north (N), west (W), south (S), and east (E) of the pool. Water was filled up to 1 cm above the platform, and the platform was placed in the center of one (SW) of the four quadrants. Learning training, a process for animals to remember the platform, was performed for 5 consecutive days, and probe tests were performed on the sixth day. All mice were trained to remember the platform for 5 days (four times a day), and the probe test was performed on the sixth day. The animals were placed in four quadrants facing the wall and were given 1 min to find the platform. Once they found the platform within 1 min, they were left on the platform for 10 s for learning. Meanwhile, animals that were unable to find the platform were placed on the platform for 10 s at the end of the session. The probe test was performed without the platform. Animals started on the wall of the quadrant zone opposite the platform, and their movements for 1 min were recorded using a tracking system (Harvard Apparatus, Holliston, MA, USA).



## **Part 2. The combined therapy of FUS and aducanumab for AD**

### **1. Animals**

As in Part 1, the 5xFAD AD mouse model was used. All mice were housed in groups of 2–5 per cage with ad libitum access to food and water, in a humidity- and temperature-controlled, specific pathogen-free environment (12-h light cycle; lights on at 8 am) at the Seoul National University College of Medicine Animal Care Facility. The animal cages were changed once a week by experimenters. All animal experiments were approved by the Animal Care Committee of Seoul National University College of Medicine using the Animal Care and Use Guidelines. Animal treatment and maintenance were approved and performed according to the Animal Care Committee of Seoul National University, Seoul, Republic of Korea (approval no.: SNU-201005-2-1).

### **2. Drug: aducanumab**

The human aducanumab antibody was produced using the Expi293 expression system by transient transfection with a vector encoding variable regions cloned into a human IgG1 framework and purified using protein A/G chromatography. Heavy-chain and light-chain sequences were identified in Biogen Idec's patent submission for WO2014089500A1.

### 3. Combined therapy of FUS and aducanumab

Six-month-old male 5xFAD mice were divided into five groups: 5xFAD, 5xFAD + aducanumab, 5xFAD + FUS, 5xFAD + FUS + aducanumab, and sham groups (n = 10–15 per group). The FUS parameters and procedures were the same as those described in Part 1. The first treatment was performed when mice were 6 months old. Each group underwent FUS treatment three times at an interval of 2 weeks (Figure 4). Aducanumab (3 mg/kg in saline) was injected intravenously at the end of FUS sonication.

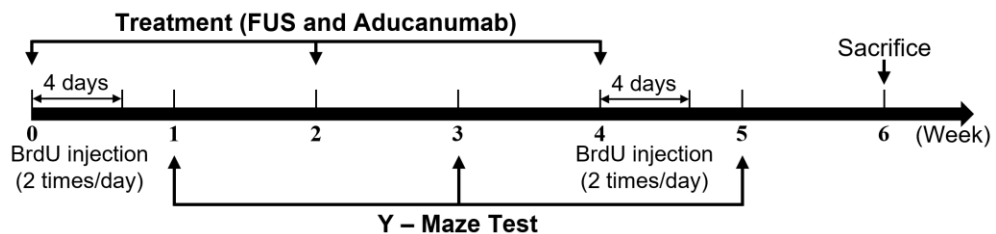


**Figure 4. Experimental timeline for combined therapy of FUS and aducanumab.**

Three FUS treatments were performed at an interval of 2 weeks. Y-maze tests were performed 1 week after each treatment.

#### **4. Magnetic resonance imaging**

To confirm the permeability of the BBB, post-T1-weighted images with gadolinium were compared to the pre-T1-weighted images without gadolinium (Figure 5A–F). T2-weighted images confirmed the safety of FUS in the absence of microbleeding and edema (Figure 5G–H). Magnetic resonance imaging (MRI) was performed immediately followed by sonication with a Bruker 9.4 T 20-cm bore MRI system (Biospec 94/20 USR; Bruker, Ettlingen, Germany) and mouse head coil (Table 2). A gadolinium-based MRI contrast agent, gadobutrol (Gd; Gadovist; 0.2 mL/kg), was injected intravenously.

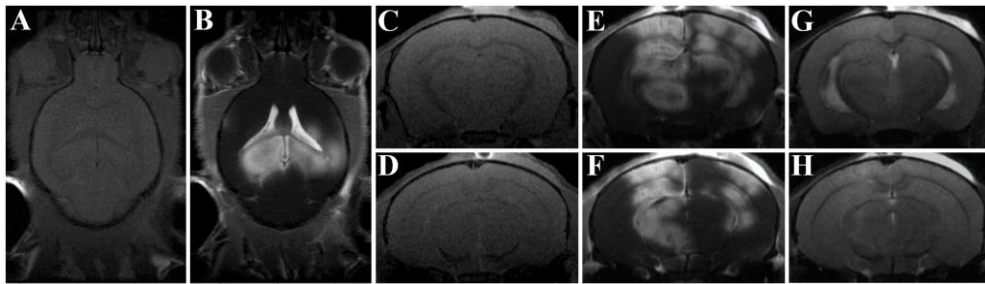


**Figure 5. Confirmation the FUS-mediated BBB opening.**

Four regions were targeted per sonication. (A–B) Transverse T1-weighted pre-/post-gadolinium MR images were taken to confirm the increase in BBB permeability. (C–D) Coronal T1-weighted pre-gadolinium MR images after FUS. (E–F) Coronal T1-weighted post-gadolinium MR images after FUS. (G–H) No clear hemorrhage or edema was observed in the coronal T2-weighted images.

**Table 2. MRI sequences and parameters**

	<b>T1-weighted imaging</b>	<b>T2-weighted imaging</b>
Echo	1	1
TR (ms)	500	2500
TE (ms)	8.1	33
FA (deg)	90	90
NEX	5	2
FOV (cm)	2 × 2	2 × 2
Matrix	256 × 256	256 × 256

## **5. Behavioral test: spontaneous alteration in the Y-maze test**

To investigate the impairment of spatial working memory, spontaneous alternation in the Y-maze was observed. The Y-maze test was performed three times 1 week after each treatment. The alternation performance was tested using a symmetrical Y-maze, consisting of three equal arms ( $40 \times 15 \times 9$  cm) and constructed using black acrylic plastic. All mice were placed at the center of the Y-maze and allowed to explore freely for 8 min. All movements were recorded using a video camera and were analyzed to determine the alternation ratio by manually evaluating the number of triads containing entries into all three arms.

## **6. BrdU labeling**

To determine whether FUS induced neurogenesis, 5-bromo-2'-deoxyuridine (BrdU) was injected intraperitoneally twice a day for 4 days 24 h after treatment. BrdU, a marker of newborn cells, is a thymidine analog that incorporates into dividing cells during the S-phase of the cell cycle.<sup>27</sup> To investigate the effects of repeated FUS treatment, differences in neurogenesis were compared between single treatment and multiple treatment groups. Half of the group was injected after the first treatment, and the remaining half was injected after the third treatment.

## 7. Immunohistochemistry

Brains were fixed in 4% paraformaldehyde for 24 h, transferred to 30% sucrose for 3 days for immunohistochemistry, and stored at  $-20^{\circ}\text{C}$  in a cryoprotectant storage solution until use. Brains were cut into 30- $\mu\text{m}$  coronal sections. Free-floating sections were washed in PBS and incubated in blocking solution (PBS, 5% normal goat serum, 0.2% Triton X100) for 3 h at room temperature. The sections were incubated with primary antibodies in blocking solution overnight at  $4^{\circ}\text{C}$ . The following primary antibodies were used for immunohistochemistry: BrdU (proliferation marker, Abcam, ab6326, rat, 1:250), NeuN (mature neuronal marker, Millipore, ABN78, rabbit, 1:500), and 6E10 (anti-human  $\text{A}\beta$  monoclonal antibody, Biolegend, SIG39320, mouse, 1:500). After the primary immunoreaction, sections were incubated with secondary antibodies conjugated with Alexa488 (Invitrogen, A11008, 1:500) and Alexa 594 (Abcam, A150156, 1:250). Immunostaining of the sections was visualized using an LSM 700 confocal microscope (Carl Zeiss, Jena, Germany) or an Axio Imager M2 (Carl Zeiss) light microscope. The number and area of plaques detected by 6E10 were quantified using ImageJ software (version 1.52a, Wayne Rasband, NIH, MD, USA).

## 8. Statistical analysis

All data were expressed as the mean  $\pm$  standard error of the mean (SEM). Data were calculated using one-way and two-way analysis of variance (ANOVA) followed by Tukey's and least significant difference post hoc analysis. The  $p$ -value  $< 0.05$  were considered statistically significant. All statistical analyses were performed using SPSS (version 25, SPSS Inc., Chicago, IL, USA) and GraphPad Prism 7 software (GraphPad Software Inc., San Diego, CA, USA).

### III. RESULTS

#### Part 1. Safety and efficiency of FUS in a 5xFAD mouse model of AD

##### 1. Examination of safety for FUS-mediated noninvasive BBB opening

To determine BBB opening efficiency and safety depending on the changes in acoustic pressure amplitude, both EB extravasation and histological tissue damage were confirmed in response to 0.22-, 0.23-, 0.24-, 0.25-MPa acoustic pressures. As a result of the BBB opening according to acoustic pressures, the transmission rate of EB was the highest at 0.25-MPa acoustic pressures (Figure 6A). Evaluation of the brain region through H&E staining revealed no damage, such as microbleeding or visible structural injuries at the targeted regions (Figure 6B).

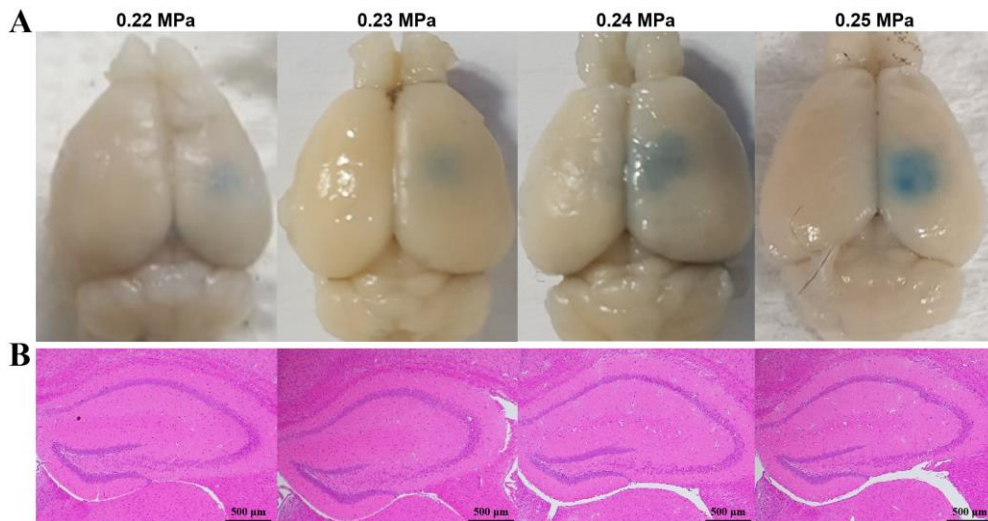


**Figure 6. Confirmation of BBB opening and evaluation of tissue damage.**

(A) Evans blue extravasation in the sonicated regions of the brain. BBB opening with increasing acoustic pressure amplitude from 0.22 MPa to 0.25 MPa. (B) The targeted brain regions were histologically evaluated by H&E staining.



## **2. FUS-induced BBB opening decreased amyloid plaques in the hippocampus.**

To determine whether FUS-mediated BBB opening affects A $\beta$  reduction, mice ( $n = 3$ ) were sacrificed 1 week after FUS treatment. The total number of A $\beta$  in the dentate gyrus (DG) of the hippocampus in the FUS-treated hemisphere was lower than that in the contralateral hippocampus (Figure 7A). The number of A $\beta$  plaques in the ipsilateral hippocampus ( $50.00 \pm 8.185$ ) was significantly lower than that in the contralateral hippocampus ( $91.00 \pm 9.849$ );  $p < 0.05$  (Figure 7B). Additionally, the total area of A $\beta$  plaques in the ipsilateral hippocampus ( $1,028 \pm 163$ ) was significantly lower than that in the contralateral hippocampus ( $2,796.00 \pm 210.70$ );  $p < 0.01$  (Figure 7C).

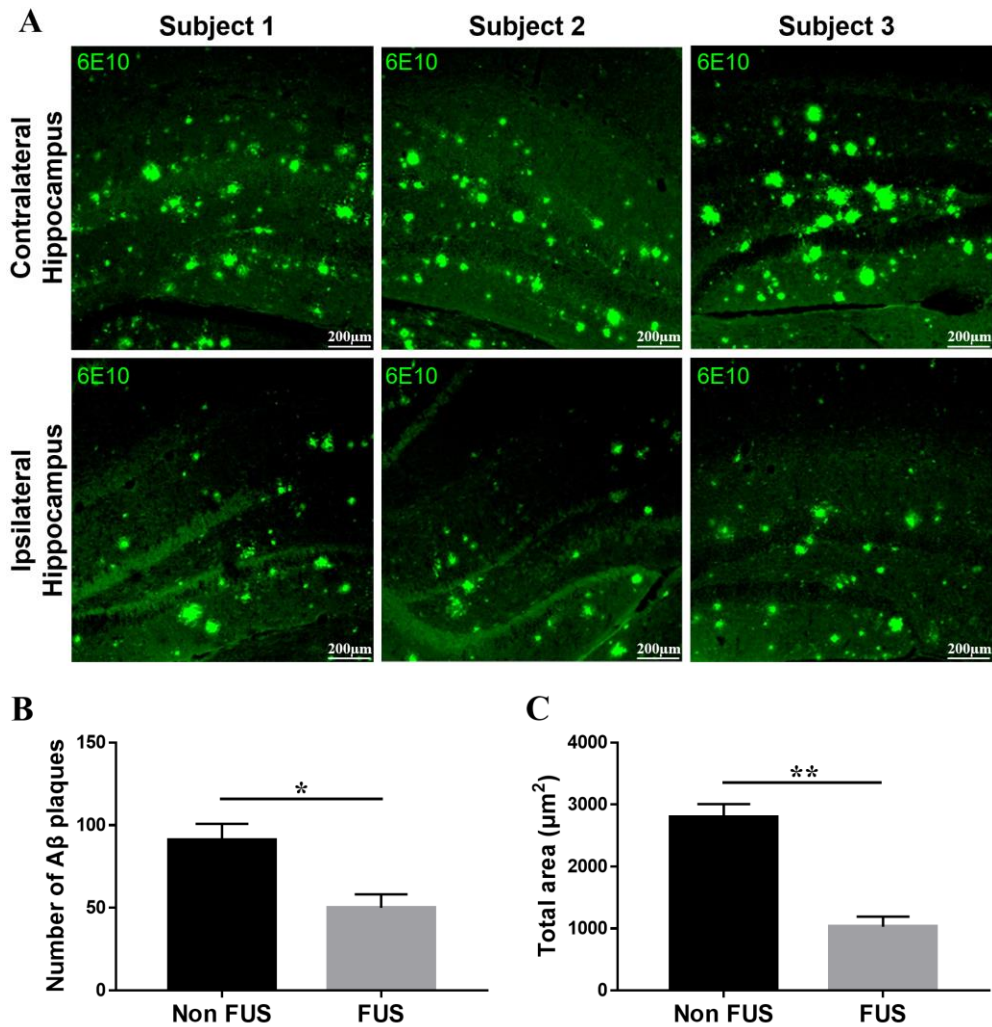


**Figure 7. FUS-mediated BBB opening reduced Aβ plaques.** (A) M2 images (10×) of Aβ-stained 6E10 antibody in the dentate gyrus (DG) of the hippocampus. (B–C) Bar graph shows the number of total Aβ plaques and total area in the DG of the hippocampus. \* $p < 0.05$ , \*\* $p < 0.01$ ,  $n = 3$ ; Unpaired t-test (two-tailed) was used for the statistical analysis.

### 3. FUS-induced BBB opening improved the cognitive function in 5xFAD

The Morris water maze test was performed to investigate the changes in cognitive function and memory following FUS treatment. Throughout the 5-day training, the time to find the platform gradually decreased in the sham, sham + FUS and TG + FUS groups (Figure 8A). In contrast, the TG group spent more time searching for and reaching the platform, indicating that they had difficulties with learning and memory. The sham ( $p < 0.0001$ ) and sham + FUS ( $p < 0.0001$ ) groups displayed significantly better memory and learning abilities than that in the TG group (Figure 8A). In the probe test, the TG group ( $0.42 \pm 0.20$ ) had a significantly fewer number of crossings than that in the sham ( $3.07 \pm 0.62$ ;  $p < 0.05$ ) and sham + FUS ( $3.72 \pm 0.54$ ;  $p < 0.01$ ) groups (Figure 8B). The TG + FUS group ( $1.02 \pm 0.24$ ) showed a significantly longer time in the platform area compared with that in the TG group ( $0.10 \pm 0.05$ );  $p < 0.01$  (Figure 8C). The amount of time spent in the quadrant zone was significantly decreased in the TG group ( $7.04 \pm 1.85$ ) compared to that in the sham ( $17.00 \pm 1.71$ ;  $p < 0.01$ ), sham + FUS ( $24.21 \pm 1.73$ ;  $p < 0.0001$ ), and TG + FUS groups ( $22.15 \pm 3.33$ ;  $p < 0.001$ ) (Figure 8D). Additionally, the mean speed in the pool was significantly slower in the TG group ( $13.62 \pm 2.52$ ) than that in the sham group ( $19.79 \pm 1.12$ );  $p < 0.05$  (Figure 8E).

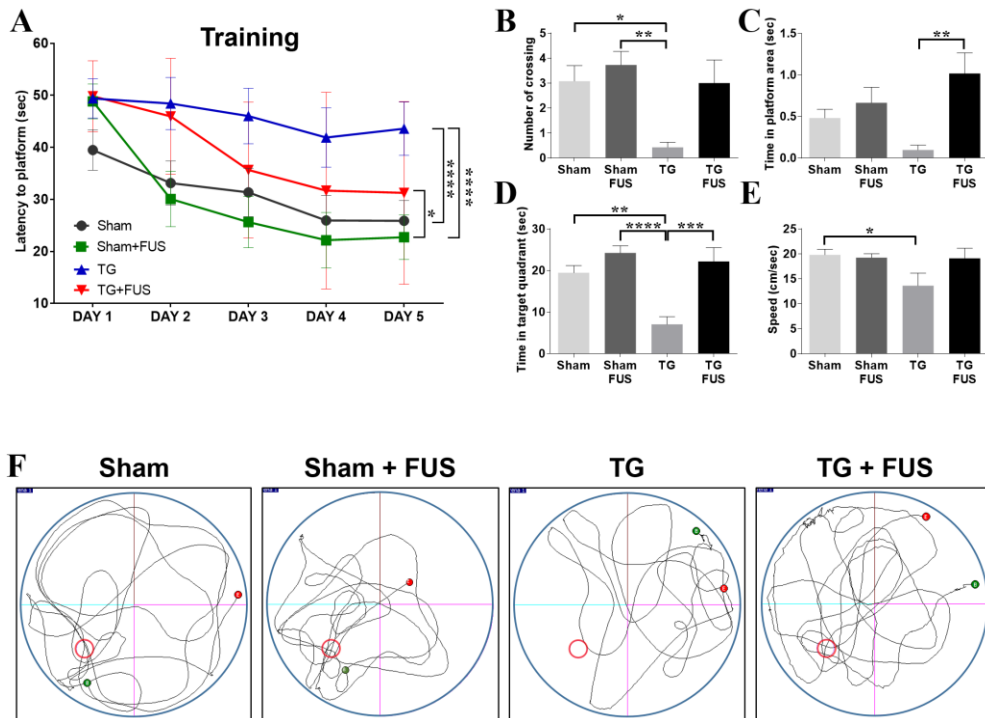


**Figure 8. FUS improves cognitive function and spatial memory.**

(A) Learning curves of the 5 consecutive days. Latency to platform means the time required for mice to find the escape platform during training trials. Data are presented means  $\pm$  standard error of the mean (SEM).  $*p < 0.05$ ,  $****p < 0.0001$ ; Two-way ANOVA with Tukey's multiple comparison test. (B–E) Results of the probe test one day after the end of the training for 1 days. Data are presented means  $\pm$  SEM.  $*p < 0.05$ ,  $**p < 0.01$ ,  $***p < 0.001$ ,  $****p < 0.0001$ ; One-way ANOVA with Tukey's multiple comparison test. (F) Trajectory maps of animals in the probe test. Groups: sham ( $n = 13$ ), sham + FUS ( $n = 11$ ), TG ( $n = 7$ ), TG + FUS ( $n = 7$ ).

## **Part 2. The combined therapy of FUS and aducanumab for AD**

### **4. The combined therapy of FUS and aducanumab rescued the cognitive impairments in 5xFAD**

The combined effect of FUS and aducanumab on spatial memory was evaluated using the Y-maze test. FUS treatment was performed three times at 2-week intervals, and the Y-maze test was performed 1 week after each treatment. As a result, compared with the 5xFAD group, alteration rates in the combined treatment group were all recovered regardless of the number of FUS treatments. In the first treatment, the combined treatment group ( $0.59 \pm 0.03$ ) featured significantly recovered alteration rates compared with that in the 5xFAD group ( $0.47 \pm 0.02$ );  $p < 0.05$  (Figure 9). In the repeated treatment, the combined treatment group ( $0.66 \pm 0.02$ ) exhibited even higher recovered alteration rates compared with that in the 5xFAD group ( $0.48 \pm 0.05$ );  $p < 0.001$  (Figure 9). Moreover, the combined treatment group featured significantly recovered alteration rates compared with the only aducanumab ( $0.55 \pm 0.03$ ;  $p < 0.04$ ) and only FUS groups ( $0.54 \pm 0.03$ ;  $p < 0.01$ ). Thus, the repeated combined treatment contributed to a more significant improvement in cognitive function than a single treatment.

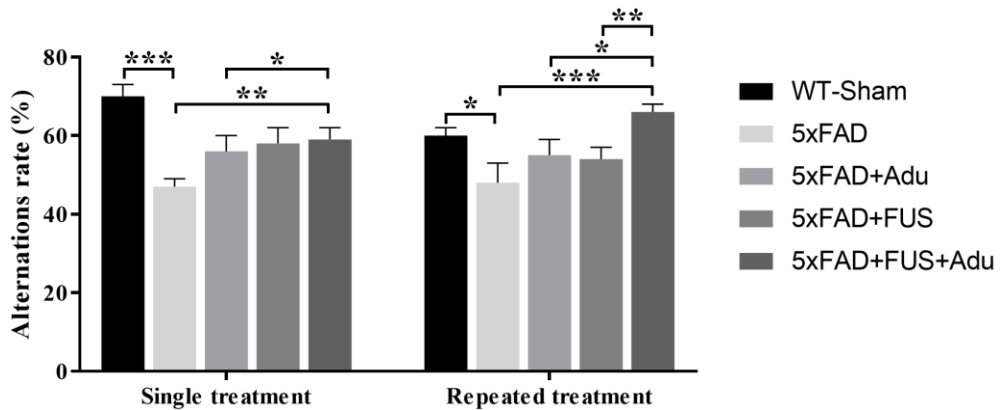


**Figure 9. The combined therapy of FUS and aducanumab restored cognitive impairments.** Bar graphs show the spontaneous alternation rate in 5xFAD mice 1 week after the first treatments (left) and 1 week after repeated treatment (right). Data were expressed as mean  $\pm$  SEM. \* $p < 0.05$ , \*\* $p < 0.01$ , \*\*\* $p < 0.001$ ; Statistical analysis was performed using one-way ANOVA followed by least significant difference analysis. Groups of single treatment: sham (n = 20), 5xFAD (n = 15), 5xFAD + Adu (n = 14), 5xFAD + FUS (n = 15), and 5xFAD + Adu + FUS (n = 22) groups. Groups of repeated treatment: sham (n = 13), 5xFAD (n = 13), 5xFAD + Adu (n = 12), 5xFAD + FUS (n = 17), and 5xFAD + Adu + FUS (n = 17) groups.

## **5. The combined therapy of FUS and aducanumab decreased amyloid plaques in the dentate gyrus of the hippocampus**

6E10, an A $\beta$  marker, was stained to determine whether the combined therapy would be more effective in reducing A $\beta$  than either FUS or aducanumab treatment alone (Figure 10A). The combined therapy group ( $2.5 \pm 0.65$ ) showed a significantly decreased number of A $\beta$  plaques  $>100 \mu\text{m}^2$  in the DG of the hippocampus compared with that in the 5xFAD group ( $10 \pm 0.78$ );  $p = 0.0003$  (Figure 10B). In A $\beta$  plaques  $<100 \mu\text{m}^2$ , the combined therapy group ( $8.33 \pm 0.93$ ) showed a significantly decreased number of A $\beta$  plaques compared with the 5xFAD group ( $19.9 \pm 2.43$ ;  $p = 0.0037$ ) (Figure 10B). No significant differences were found in the number of A $\beta$  plaques  $>100 \mu\text{m}^2$  in the DG of the hippocampus in the FUS ( $6 \pm 0.7$ ) and aducanumab groups ( $6.57 \pm 1.04$ ) compared with that in the 5xFAD group ( $10 \pm 0.78$ ) (Figure 10B). No significant differences were found in the number of A $\beta$  plaques  $<100 \mu\text{m}^2$  in the DG of the hippocampus in the FUS ( $15.12 \pm 1.56$ ) and aducanumab groups ( $15.28 \pm 2.12$ ) compared with that in the 5xFAD group ( $19.9 \pm 2.43$ ) (Figure 10B). The total area of the A $\beta$  plaques in the DG of the hippocampus significantly decreased in the combined treatment group (A $\beta > 100 \mu\text{m}^2$ ,  $495.29 \pm 172.99$ ;  $p < 0.0002$ ; A $\beta < 100 \mu\text{m}^2$ ,  $298.58 \pm 14.14$ ;  $p < 0.0064$ ) compared with that in the 5xFAD group (A $\beta > 100 \mu\text{m}^2$ ,  $2841.02 \pm 328.38$ ; A $\beta < 100 \mu\text{m}^2$ ,  $653.85 \pm 91.60$ ) (Figure 10C). A significant difference was not observed in the FUS (A $\beta > 100 \mu\text{m}^2$ ,  $1421.71 \pm 182.44$ ; A $\beta < 100 \mu\text{m}^2$ ,  $484.06 \pm 50.73$ ) and aducanumab groups (A $\beta > 100 \mu\text{m}^2$ ,  $1754.28 \pm 296.52$ ; A $\beta < 100 \mu\text{m}^2$ ,  $556.71 \pm 74.25$ ) compared with that in the 5xFAD group (A $\beta > 100 \mu\text{m}^2$ ,  $2841.02 \pm 328.38$ ; A $\beta < 100 \mu\text{m}^2$ ,  $653.85 \pm 91.60$ ) (Figure 10C).

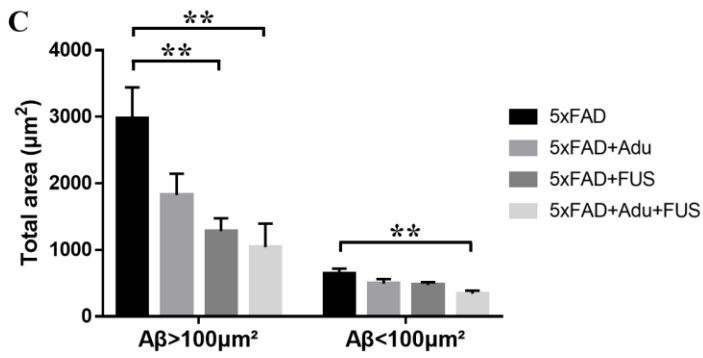
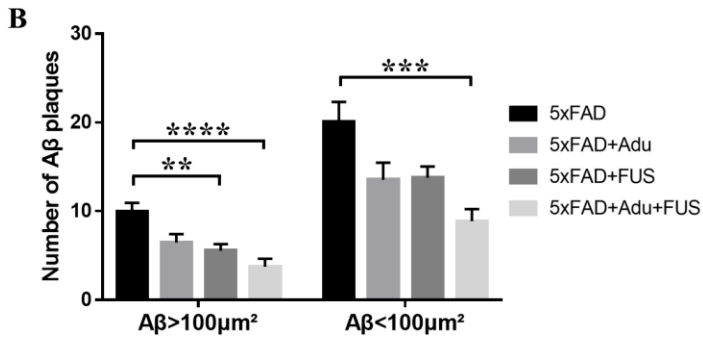
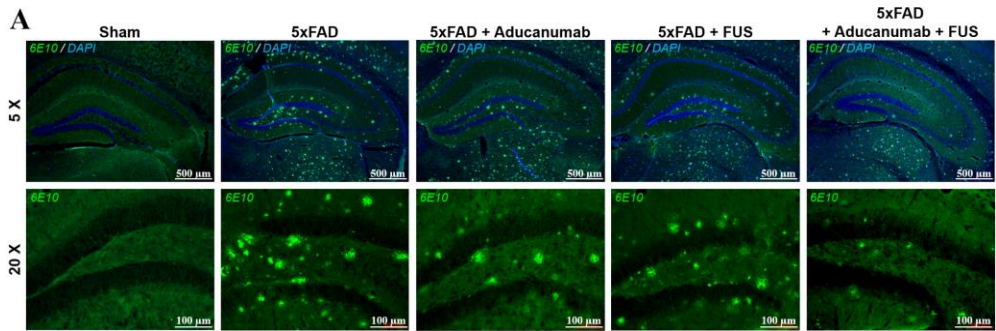




**Figure 10. Combined therapy of FUS and aducanumab decreased A $\beta$  accumulation in 5xFAD mice.** (A) Above, representative M2 images (5 $\times$ ) of A $\beta$ -stained 6E10 antibody and DAPI in the hippocampus. (A) Below, representative M2 images (20 $\times$ ) of A $\beta$ -stained 6E10 antibody in the dentate gyrus (DG) of the hippocampus. (B) Bar graph shows the number of A $\beta$  plaque >100  $\mu\text{m}^2$  and <100  $\mu\text{m}^2$  in the DG of the hippocampus. (C) Bar graph shows the total area of A $\beta$  plaque >100  $\mu\text{m}^2$  and <100  $\mu\text{m}^2$  in the DG of the hippocampus. Data are presented means  $\pm$  SEM. \*\* $p < 0.01$ , \*\*\* $p < 0.001$ , \*\*\*\* $p < 0.0001$ ; One-way ANOVA with Tukey's multiple comparison test. Groups: 5xFAD (n = 13), 5xFAD + Adu (n = 11), 5xFAD + FUS (n = 13), and 5xFAD + Adu + FUS (n = 15).

## **6. The combined therapy of FUS and aducanumab increased neurogenesis in 5xFAD mouse**

To confirm the effects of proliferation and neurogenesis, the stained BrdU and NeuN in the subgranular zone and granular cell layer of the DG were quantified (Figure 11A). The number of BrdU<sup>+</sup> and BrdU<sup>+</sup>/NeuN represents the average of seven sections, serially sectioned at 30- $\mu$ m intervals of the hippocampus.

In the single treatment, the number of BrdU-positive cells was significantly increased in the combined therapy group ( $7.92 \pm 1.19$ ) compared with that in the 5xFAD ( $2.19 \pm 0.36$ ;  $p < 0.001$ ), 5xFAD + Adu ( $4.45 \pm 0.87$ ;  $p < 0.05$ ), and 5xFAD + FUS ( $4.09 \pm 1.02$ ;  $p < 0.05$ ) groups (Figure 11B). Meanwhile, the bar graphs show a significantly decreased number of BrdU-positive cells in the 5xFAD group ( $2.19 \pm 0.36$ ) compared with that in the sham group ( $5.35 \pm 1.22$ );  $p < 0.05$  (Figure 11B). For BrdU<sup>+</sup>/NeuN double-labeled cells, the combined therapy group ( $4.18 \pm 0.62$ ) also exhibited a higher number of BrdU<sup>+</sup>/NeuN double-labeled cells compared with that in the 5xFAD group ( $1.17 \pm 0.24$ );  $p < 0.01$  (Figure 11B), whereas the 5xFAD group ( $1.17 \pm 0.24$ ) had a significantly decreased number of BrdU<sup>+</sup>/NeuN double-labeled cells compared with that in the sham group ( $3.71 \pm 1.13$ );  $p < 0.01$  (Figure 11B).

In the repeated treatment, the effectiveness was consistent with the results of the single treatment. The number of BrdU-positive cells was significantly increased in the combined therapy group ( $8.10 \pm 0.29$ ) compared with that in the 5xFAD ( $3.76 \pm 0.71$ ;  $p < 0.05$ ) and sham ( $4.57 \pm 0.44$ ;  $p < 0.05$ ) groups (Figure 11C). The bar graphs showed a significantly increased number of BrdU-positive cells in the 5xFAD + FUS group ( $9.27 \pm 1.98$ ) compared with that in the sham ( $4.57 \pm 0.44$ ;  $p < 0.01$ ), 5xFAD ( $3.76 \pm 0.71$ ;  $p < 0.01$ ), and 5xFAD + Adu ( $5.06 \pm 0.99$ ;  $p < 0.05$ ) groups (Figure 11C). The combined therapy group ( $3.70 \pm 0.34$ ) also exhibited a higher number of

BrdU<sup>+</sup>/NeuN double-labeled cells compared with that in the 5xFAD group ( $1.83 \pm 0.27$ );  $p < 0.05$  (Figure 11C). Moreover, a significantly increased number of BrdU<sup>+</sup>/NeuN double-labeled cells was observed in the 5xFAD + FUS group ( $4.04 \pm 0.93$ ) compared with that in the sham ( $2.42 \pm 0.29$ ;  $p < 0.01$ ), 5xFAD ( $1.83 \pm 0.27$ ;  $p < 0.05$ ) groups (Figure 11C).

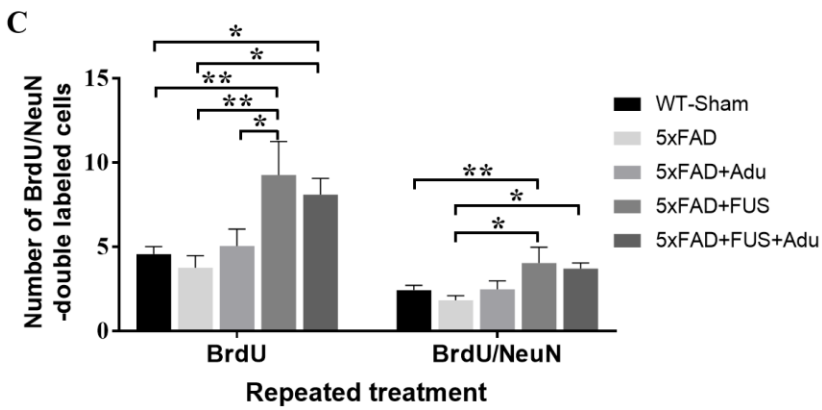
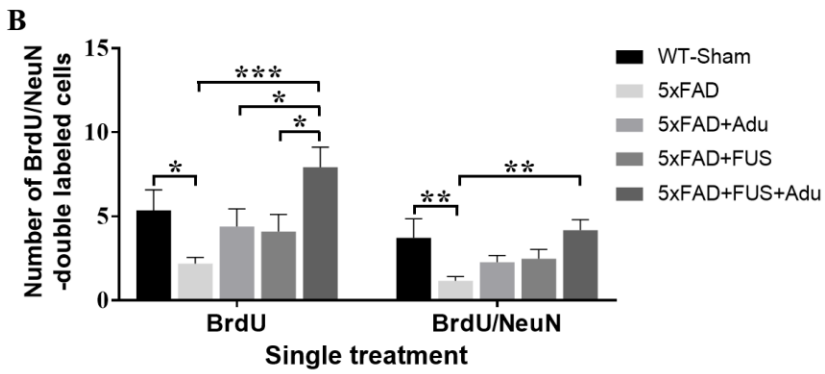
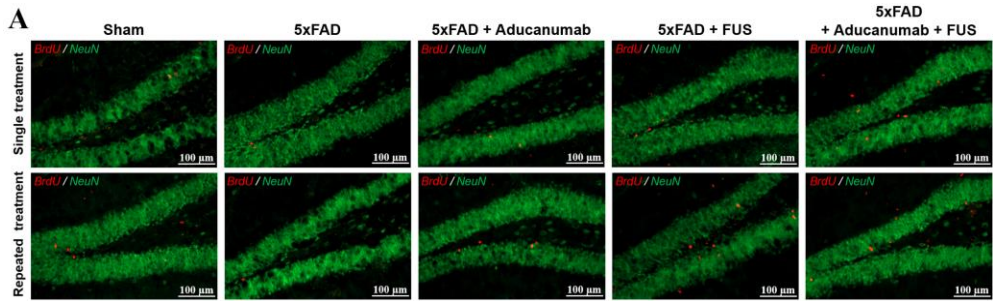


**Figure 11. Analysis of cell proliferation and neurogenesis in the DG of the hippocampus.** (A) Representative images showing immunofluorescence of neuronal nuclear antigen (NeuN, green), 5-bromo-2'-deoxyuridine (BrdU, red), or their colocalization (BrdU/NeuN). Scale bars: 100  $\mu$ m. (B) A number of BrdU and BrdU/NeuN-positive cells in the hippocampal dentate gyrus (DG) with a single treatment. Groups: sham (n = 8), 5xFAD (n = 8), 5xFAD + Adu (n = 6), 5xFAD + FUS (n = 6), and 5xFAD + Adu + FUS (n = 7). (C) The number of BrdU and BrdU/NeuN-positive cells in the hippocampal DG with repeated treatments. Groups: sham (n = 10), 5xFAD (n = 6), 5xFAD + Adu (n = 5), 5xFAD + FUS (n = 8), and 5xFAD + Adu + FUS (n = 7). Data are expressed as mean  $\pm$  SEM. \* $p$  < 0.05, \*\* $p$  < 0.01, \*\*\* $p$  < 0.001; Statistical analysis was performed using one-way ANOVA followed by least significant difference post hoc analysis.

## IV. DISCUSSION

This study aimed to demonstrate the fundamental AD treatment effects by reducing A $\beta$  aggregation through the application of FUS with antibody therapy in a 5xFAD AD mouse model. In recent years, preclinical and clinical studies using FUS have been actively conducted around the world, and their use in clinical practice has gradually become increasingly stable and safe.<sup>16,28,29</sup> Although there have been several attempts to combine FUS with other therapeutic strategies, it has been challenging to secure safety as well as effectiveness at a time.<sup>30-32</sup> However, this study may provide some insight into the development of a novel therapeutic strategy for AD. For many of the treatments for neurodegenerative diseases, it is important that the drugs travel down to the target region, but the BBB mostly hinders the molecules from reaching the target in the brain, thereby making the potentially effective therapy ineffective. Commonly, only lipophilic molecules with a small molecular weight (under 400–600 Da) can cross the BBB.<sup>33</sup> Monoclonal antibodies have a therapeutic potential for treating neurodegenerative diseases, but their delivery in the brain is limited by the BBB due to its large molecular weight.<sup>34</sup> The weight of aducanumab used in this study is 146 kDa, which normally cannot pass through the BBB without any kind of modulation. Therefore, with regard to its effectiveness, treatment with antibody therapy alone is marginal or infeasible. However, it is believed that FUS could not only resolve these drawbacks of antibody therapy but also show the synergistic effects of FUS and antibody therapy.

To address these fundamental issues, the therapeutic effects were analyzed from three perspectives: A $\beta$  accumulation, decline of cognitive function, and the occurrence of adult hippocampal neurogenesis. In this study, the combined therapy

of FUS and aducanumab was confirmed to have significant effects on the recovery of cognitive function, A $\beta$  reduction, and neurogenesis. In AD, cognitive function is severely impaired and considered to be one of the most common symptoms. As shown in the behavioral tests, 5xFAD mice that did not undergo any treatment showed significantly lower alteration rates than that in other treatment groups. These results prove that even a single FUS treatment can enhance memory function, but multiple treatments greatly augment its effectiveness. Further, neurogenesis in the target area has increased where FUS was sonicated, stating that it may have served to increase cognitive function.

Since Hynynen et al. reported that FUS-mediated BBB opening induces hippocampal neurogenesis, numerous follow-up studies have been conducted.<sup>22,23,35,36</sup> However, the mechanism by which FUS induces neurogenesis has not yet been clearly elucidated. This study demonstrated that neurogenesis only occurs when FUS-mediated BBB opening occurs. Since neurogenesis is induced only when the BBB is opened, it is assumed that changes in the intravascular microenvironment or the components of the tight junction may have played a role in promoting neurogenesis. In addition, the brain-derived neurotrophic factor (BDNF) is one of the most important factors in neurogenesis,<sup>37</sup> and a report revealed that FUS-mediated BBB opening increases BDNF.<sup>23</sup> Therefore, these results could be in line with those of previous studies and contribute to understanding the mechanism of FUS and neurogenesis.

Doublecortin (DCX; marker of neurogenesis) was examined using immunohistochemistry, but this was not presented in this study. At the beginning of the experiment, mice were 6 months old, and the time point of sacrifice was when mice turned 8 months. The expression of DCX in all groups was hardly observed.<sup>38</sup>

In modern medicine, the development of new pharmaceuticals for numerous brain treatments, including AD, has been delayed because all large-molecule pharmaceuticals cannot penetrate the BBB. Aducanumab is also a large-molecule pharmaceutical that can hardly cross the BBB and has a dose-dependent therapeutic effect only when the BBB is functionally disrupted. For this reason, aducanumab has been administered at a high dose, causing side effects such as amyloid-related imaging abnormalities, headache, and urinary tract infection.<sup>8</sup> In another study using transgenic mice (Tg2576), A $\beta$  was significantly reduced in the group given a dose of  $\geq 10$  mg/kg, and at the 0.3–3 mg/kg dose, A $\beta$  did not decrease significantly.<sup>8</sup> When aducanumab is administered at a high dose, the effect of A $\beta$  reduction has been shown to be evident. However, because the probability of side effects increases significantly, a strategy to reduce the dose and increase the effectiveness is needed.

When FUS was treated unilaterally with aducanumab, aducanumab was expressed only in the ipsilateral hemisphere, and the expression increased depending on the dose (Figure 12). Aducanumab is normally expressed at 146 kDa, as mentioned above. However, in vivo generation of the aducanumab antibody may vary slightly as glycosylation occurs.



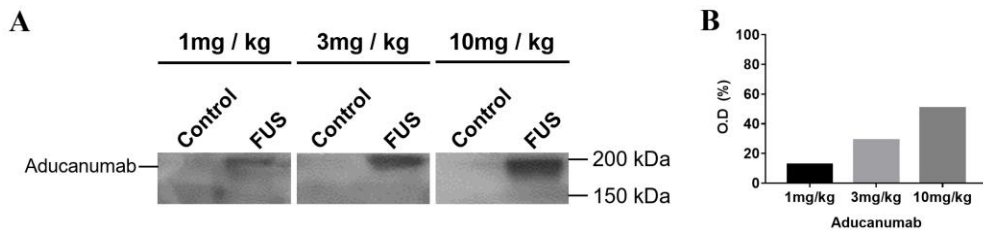


**Figure 12. Dose dependent aducanumab expression level delivered by FUS.**

(A) Representative images present dose-dependent aducanumab expression in the FUS-sonicated brain. Aducanumab was not expressed in the hemisphere not sonicated with FUS. (B) Expression rates (1 mg/kg, 12.52%; 3 mg/kg, 20.05%; 10 mg/kg, 50.63%) of dose-dependent aducanumab after FUS-mediated BBB opening.

FUS plays an important role in increasing the delivery rate of aducanumab into the brain to reduce amyloid plaques. The results of this study suggest that FUS not only contributes to the increase in BBB permeability, but also has the ability to directly reduce amyloid plaques. Accumulating evidence consistently reported that FUS reduced amyloid plaques, but its mechanism remained unclear.<sup>39-43</sup> Previous studies suggested increases in endogenous immunoglobulins binding to A $\beta$  plaques with FUS-mediated BBB opening.<sup>40</sup> In addition, they reported that FUS increased microglia and astrocytes in relation to A $\beta$  phagocytosis, which remains controversial.<sup>40</sup> As microglia are the main phagocytes in the central nervous system, it is more likely to rapidly decrease in A $\beta$  plaques. It is also possible that FUS induces infiltration of systemic phagocytic immune cells, which may also aid in A $\beta$  reduction. Furthermore, FUS has recently been shown to induce an increase in monocyte chemoattractant protein-1 and migration of CD68<sup>+</sup> systemic macrophages.<sup>44,45</sup>

In this study, A $\beta$  was not significantly decreased in the group treated with aducanumab alone, and A $\beta$  was significantly decreased when administered with FUS. A positive treatment strategy of using a low dose of 3 mg/kg rather than a high dose of 10 mg/kg or more has been suggested, even by increasing the drug delivery rate to the target using FUS. Although the efficacy of aducanumab has been demonstrated in current clinical studies, it faced difficulties with disapproval in phase 3 clinical trials due to side effects caused by high doses. Recently, aducanumab has received FDA approval. Although it has shortcomings in terms of efficacy and side effects, it is believed to overcome barriers to FUS.

There are still uncertainties about the benefits of aducanumab, and additional clinical trials are needed to confirm the efficacy of the drug. However, this study is the first to demonstrate that combined treatment with FUS and antibody therapy can

directly reduce A $\beta$  plaques and enhance cognitive functions as well as neurogenesis. Currently, AD patients desperately need treatment to delay disease progression, but this study presented the possibility of targeting the fundamental issues of AD.

## V. CONCLUSION

This study aimed to demonstrate the effects of FUS and aducanumab in an AD mouse model and propose the potential of the combined therapy for AD treatment. In part 1, safe and efficient parameters of FUS in the 5xFAD AD mouse model were established. Consequently, a safe parameter that could maximize the effectiveness of FUS was secured. The FUS-treated group showed remarkably decreased levels of A $\beta$  plaques without any hemorrhages or edema, and it was shown that FUS promoted cognitive function. Part 2 shows that the combined therapy significantly reduced A $\beta$  plaques and restored cognitive function compared to either FUS or aducanumab treatment alone. Moreover, the combined therapy significantly induced proliferation and neurogenesis. Interestingly, even a low dose of aducanumab was shown to be effective, whereas previous studies reported that only a high dose of aducanumab was effective. These data indicate that FUS increased the permeability of the BBB and enabled drugs to pass through the barrier without any side effects, which is the most controversial issue and downside of drug delivery. Overall, the potential of the combined therapy would provide insight into establishing a novel therapeutic strategy for the treatment of AD as well as other neurodegenerative diseases.

## REFERENCES

1. Graham WV, Bonito-Oliva A, Sakmar TP. Update on Alzheimer's disease therapy and prevention strategies. *Annual review of medicine* 2017;68:413-30.
2. Cummings J, Lee G, Ritter A, Sabbagh M, Zhong K. Alzheimer's disease drug development pipeline: 2020. *Alzheimer's & Dementia: Translational Research & Clinical Interventions* 2020;6:e12050.
3. Cummings J, Lee G, Zhong K, Fonseca J, Taghva K. Alzheimer's disease drug development pipeline: 2021. *Alzheimer's & Dementia: Translational Research & Clinical Interventions* 2021;7:e12179.
4. Kim HY, Kim HV, Jo S, Lee CJ, Choi SY, Kim DJ, et al. EPPS rescues hippocampus-dependent cognitive deficits in APP/PS1 mice by disaggregation of amyloid- $\beta$  oligomers and plaques. *Nature communications* 2015;6:1-14.
5. Madav Y, Wairkar S, Prabhakar B. Recent therapeutic strategies targeting beta amyloid and tauopathies in Alzheimer's disease. *Brain research bulletin* 2019;146:171-84.
6. Morgan D. Immunotherapy for Alzheimer's disease. *Journal of internal medicine* 2011;269:54-63.
7. Yang SH, Lee DK, Shin J, Lee S, Baek S, Kim J, et al. Nec-1 alleviates cognitive impairment with reduction of A $\beta$  and tau abnormalities in APP/PS 1 mice. *EMBO molecular medicine* 2017;9:61-77.
8. Sevigny J, Chiao P, Bussière T, Weinreb PH, Williams L, Maier M, et al. The antibody aducanumab reduces A $\beta$  plaques in Alzheimer's disease. *Nature* 2016;537:50-6.
9. Dunn B, Stein P, Cavazzoni P. Approval of Aducanumab for Alzheimer Disease—the FDA's Perspective. *JAMA Internal Medicine* 2021.
10. Karlawish J, Grill JD. The approval of Aduhelm risks eroding public trust in Alzheimer research and the FDA. *Nature Reviews Neurology* 2021:1-2.
11. Abbott NJ, Patabendige AA, Dolman DE, Yusof SR, Begley DJ. Structure and function of the blood-brain barrier. *Neurobiology of disease* 2010;37:13-25.
12. Pardridge WM. The blood-brain barrier: bottleneck in brain drug development. *NeuroRx* 2005;2:3-14.
13. Hynynen K, McDannold N, Vykhodtseva N, Jolesz FA. Noninvasive MR imaging-guided focal opening of the blood-brain barrier in rabbits. *Radiology* 2001;220:640-6.
14. Hynynen K, McDannold N, Sheikov NA, Jolesz FA, Vykhodtseva N. Local and reversible blood-brain barrier disruption by noninvasive focused ultrasound at frequencies suitable for trans-skull sonications. *Neuroimage* 2005;24:12-20.
15. Alli S, Figueiredo CA, Golbourn B, Sabha N, Wu MY, Bondoc A, et al. Brainstem blood brain barrier disruption using focused ultrasound: A demonstration of feasibility and enhanced doxorubicin delivery. *Journal of controlled release* 2018;281:29-41.
16. Park SH, Kim MJ, Jung HH, Chang WS, Choi HS, Rachmilevitch I, et al. Safety and feasibility of multiple blood-brain barrier disruptions for the treatment of glioblastoma in patients undergoing standard adjuvant chemotherapy. *Journal of neurosurgery* 2020;134:475-83.
17. Park SH, Kim MJ, Jung HH, Chang WS, Choi HS, Rachmilevitch I, et al. One-Year

- Outcome of Multiple Blood–Brain Barrier Disruptions With Temozolomide for the Treatment of Glioblastoma. *Frontiers in Oncology* 2020;10:1663.
18. Alkins R, Burgess A, Kerbel R, Wels WS, Hynynen K. Early treatment of HER2-amplified brain tumors with targeted NK-92 cells and focused ultrasound improves survival. *Neuro-oncology* 2016;18:974-81.
  19. Lee J, Chang WS, Shin J, Seo Y, Kong C, Song B-W, et al. Non-invasively enhanced intracranial transplantation of mesenchymal stem cells using focused ultrasound mediated by overexpression of cell-adhesion molecules. *Stem cell research* 2020;43:101726.
  20. Kobus T, Zervantonakis IK, Zhang Y, McDannold NJ. Growth inhibition in a brain metastasis model by antibody delivery using focused ultrasound-mediated blood-brain barrier disruption. *Journal of Controlled Release* 2016;238:281-8.
  21. Leinenga G, Götz J. Safety and efficacy of scanning ultrasound treatment of aged APP23 mice. *Frontiers in neuroscience* 2018;12:55.
  22. Mooney SJ, Shah K, Yeung S, Burgess A, Aubert I, Hynynen K. Focused ultrasound-induced neurogenesis requires an increase in blood-brain barrier permeability. *PloS one* 2016;11:e0159892.
  23. Shin J, Kong C, Lee J, Choi BY, Sim J, Koh CS, et al. Focused ultrasound-induced blood-brain barrier opening improves adult hippocampal neurogenesis and cognitive function in a cholinergic degeneration dementia rat model. *Alzheimer's research & therapy* 2019;11:1-15.
  24. Oakley H, Cole SL, Logan S, Maus E, Shao P, Craft J, et al. Intraneuronal  $\beta$ -Amyloid Aggregates, Neurodegeneration, and Neuron Loss in Transgenic Mice with Five Familial Alzheimer's Disease Mutations: Potential Factors in Amyloid Plaque Formation. *The Journal of Neuroscience* 2006;26:10129-40.
  25. Devi L, Ohno M. Phospho-eIF2 $\alpha$  level is important for determining abilities of BACE1 reduction to rescue cholinergic neurodegeneration and memory defects in 5XFAD mice. *PLoS One* 2010;5:e12974.
  26. Eimer WA, Vassar R. Neuron loss in the 5XFAD mouse model of Alzheimer's disease correlates with intraneuronal A $\beta$ 42 accumulation and Caspase-3 activation. *Molecular Neurodegeneration* 2013;8:2.
  27. Arguello AA, Harburg GC, Schonborn JR, Mandyam CD, Yamaguchi M, Eisch AJ. Time course of morphine's effects on adult hippocampal subgranular zone reveals preferential inhibition of cells in S phase of the cell cycle and a subpopulation of immature neurons. *Neuroscience* 2008;157:70-9.
  28. Lipsman N, Meng Y, Bethune AJ, Huang Y, Lam B, Masellis M, et al. Blood–brain barrier opening in Alzheimer's disease using MR-guided focused ultrasound. *Nature communications* 2018;9:1-8.
  29. Mainprize T, Lipsman N, Huang Y, Meng Y, Bethune A, Ironside S, et al. Blood-brain barrier opening in primary brain tumors with non-invasive MR-guided focused ultrasound: a clinical safety and feasibility study. *Scientific reports* 2019;9:1-7.
  30. Thomsen GM, Gowing G, Latter J, Chen M, Vit J-P, Staggenborg K, et al. Delayed disease onset and extended survival in the SOD1G93A rat model of amyotrophic lateral sclerosis after suppression of mutant SOD1 in the motor cortex. *Journal of Neuroscience* 2014;34:15587-600.
  31. Thomsen GM, Avalos P, Ma AA, Alkaslasi M, Cho N, Wyss L, et al. Transplantation of neural progenitor cells expressing glial cell line-derived neurotrophic factor into the motor cortex as a strategy to treat amyotrophic lateral sclerosis. *Stem Cells* 2018;36:1122-31.

32. Fan C-H, Ting C-Y, Lin CY, Chan H-L, Chang Y-C, Chen Y-Y, et al. Noninvasive, targeted and non-viral ultrasound-mediated GDNF-plasmid delivery for treatment of Parkinson's disease. *Scientific reports* 2016;6:1-11.
33. Bellettato CM, Scarpa M. Possible strategies to cross the blood–brain barrier. *Italian journal of pediatrics* 2018;44:127-33.
34. Bien-Ly N, Boswell CA, Jeet S, Beach TG, Hoyte K, Luk W, et al. Lack of widespread BBB disruption in Alzheimer's disease models: focus on therapeutic antibodies. *Neuron* 2015;88:289-97.
35. Scarcelli T, Jordão JF, O'reilly MA, Ellens N, Hynynen K, Aubert I. Stimulation of hippocampal neurogenesis by transcranial focused ultrasound and microbubbles in adult mice. *Brain stimulation* 2014;7:304-7.
36. Dubey S, Heinen S, Krantic S, McLaurin J, Branch DR, Hynynen K, et al. Clinically approved IVIg delivered to the hippocampus with focused ultrasound promotes neurogenesis in a model of Alzheimer's disease. *Proceedings of the National Academy of Sciences* 2020;117:32691-700.
37. Rossi C, Angelucci A, Costantin L, Braschi C, Mazzantini M, Babbini F, et al. Brain-derived neurotrophic factor (BDNF) is required for the enhancement of hippocampal neurogenesis following environmental enrichment. *European Journal of Neuroscience* 2006;24:1850-6.
38. Ziegler-Waldkirch S, d' Errico P, Sauer JF, Erny D, Savanthrapadian S, Loreth D, et al. Seed-induced A $\beta$  deposition is modulated by microglia under environmental enrichment in a mouse model of Alzheimer's disease. *The EMBO journal* 2018;37:167-82.
39. Hsu P-H, Lin Y-T, Chung Y-H, Lin K-J, Yang L-Y, Yen T-C, et al. Focused ultrasound-induced blood-brain barrier opening enhances GSK-3 inhibitor delivery for amyloid-beta plaque reduction. *Scientific reports* 2018;8:1-9.
40. Jordão JF, Thévenot E, Markham-Coultes K, Scarcelli T, Weng Y-Q, Xhima K, et al. Amyloid- $\beta$  plaque reduction, endogenous antibody delivery and glial activation by brain-targeted, transcranial focused ultrasound. *Experimental neurology* 2013;248:16-29.
41. Jordão JF, Ayala-Grosso CA, Markham K, Huang Y, Chopra R, McLaurin J, et al. Antibodies targeted to the brain with image-guided focused ultrasound reduces amyloid- $\beta$  plaque load in the TgCRND8 mouse model of Alzheimer's disease. *PloS one* 2010;5:e10549.
42. Poon CT, Shah K, Lin C, Tse R, Kim KK, Mooney S, et al. Time course of focused ultrasound effects on  $\beta$ -amyloid plaque pathology in the TgCRND8 mouse model of Alzheimer's disease. *Scientific reports* 2018;8:1-11.
43. D'Haese P-F, Ranjan M, Song A, Haut MW, Carpenter J, Dieb G, et al.  $\beta$ -Amyloid Plaque Reduction in the Hippocampus After Focused Ultrasound-Induced Blood–Brain Barrier Opening in Alzheimer's Disease. *Frontiers in Human Neuroscience* 2020;14:422.
44. Kovacs ZI, Kim S, Jikaria N, Qureshi F, Milo B, Lewis BK, et al. Disrupting the blood–brain barrier by focused ultrasound induces sterile inflammation. *Proceedings of the National Academy of Sciences* 2017;114:E75-E84.
45. McMahon D, Hynynen K. Acute inflammatory response following increased blood-brain barrier permeability induced by focused ultrasound is dependent on microbubble dose. *Theranostics* 2017;7:3989.

## ABSTRACT (IN KOREAN)

### 알츠하이머 마우스 모델에서 집속초음파와 아두카누맙의 병합 처치를 통한 베타 아밀로이드 플라크 감소 및 신경발생 유도에 의한 치료효과 검증

<지도교수 장 진 우>

연세대학교 대학원 의학과

공 찬 호

집속초음파는 미세기포와 함께 사용되어 비침습적으로 뇌혈관장벽을 제어하고 뇌 내로 약물을 전달할 수 있다. 집속초음파를 통한 뇌혈관장벽의 제어는 뇌 내로 약물 전달이 가능하게 할 뿐만 아니라 신경발생이나 면역, 다양한 환경변화를 조절할 수 있다는 전임상 연구들이 보고되었으며, 최근 치매환자를 대상으로 집속초음파 임상시험이 시작되었다. 베타 아밀로이드 침착은 치매에서 나타나는 대표적인 병리학적 현상이다. 치매 치료 전략으로써 베타 아밀로이드가 적절한지에 대해서는 아직도 많은 논란과 의문이 남아있지만, 이를 타겟으로 많은 치료 연구들이 진행중에 있다. 최근 집속초음파를 통한 뇌혈관 장벽의 제어가 뇌 내 침착된 아밀로이드 플라크를 줄여준다는 보고가 있었다. 한편 치매치료제 개발에 있어 이전에는 증상을 완화시키고 지연시키는 목적에 국한되었다면, 최근에는 병의 근본적인 원인을 해결할 수 있는 치료제를 개발하는 추세이다. 아두카누맙은 인간



단일클론항체 치료제로써 약물의 용량에 따라 치매 환자의 뇌 내 아밀로이드 플라크를 줄여주는 치료 효과가 확인되어 근본적인 치매 치료제로 여겨진다. 하지만 아두카누맙 역시 큰 분자량으로 뇌혈관장벽을 투과하기 어렵기 때문에 임상에서는 고용량을 사용하며 이는 다양한 부작용을 일으킬 수 있다. 본 연구의 최종 목적은 집속초음파와 아두카누맙의 병합 치료를 통해 신개념 치매 치료효과를 검증하는 것이다.

본 연구의 1부에서는 5xFAD 치매 마우스 모델을 이용하여 집속초음파를 통한 뇌혈관 장벽 제어의 안전성과 효율을 확인하였다. H&E 염색을 통해 뇌 내 미세손상이 발생하지 않는 안전한 파라미터를 구축하였다. 집속초음파에 의해 아밀로이드 플라크가 감소함을 면역조직화학염색을 통해 확인하고, 모리스 수중 미로 실험을 통해 인지기능이 개선됨을 확인함으로써 집속초음파가 치매 치료 수단으로서의 가능성을 확인하였다.

2부에서는 앞서 확립한 집속초음파 파라미터를 기반으로, 아두카누맙 치료제와 병합 치료에 대해 연구하였다. 연구를 위해 5xFAD, 5xFAD + 집속초음파, 5xFAD + 아두카누맙, 5xFAD + 집속초음파 + 아두카누맙, 대조군 총 5개 그룹으로 나누어 진행하였다. 집속초음파는 뇌 내 해마 영역의 4개 부위를 조사하였으며, 치료는 2주 간격으로 총 3번 실시하였다. 인지기능 회복을 조사하기 위해 Y자 미로 테스트를 수행하였으며, 아밀로이드 플라크와 신경발생 변화를 조사하기 위해 면역조직화학염색을 수행하였다. 실험결과 집속초음파와 아두카누맙을 병합치료한 그룹에서 유의하게 인지기능이 회복되고, 아밀로이드 플라크가 감소하며, 신경발생이 유도되는 효과를 확인하였다. 또한 단회 치료보다 반복 치료했을 경우 인지기능 회복이 더 증가하였다.

본 연구에서는 집속초음파를 통해 뇌 내 투과율을 증가시킴으로써

치료제를 적은 용량으로 효과를 극대화 시킬 수 있게 하며, 부작용을 최소화할 수 있다는 장점을 제시한다. 또한 뇌혈관장벽에 의해 사용이 제한되는 항체치료제의 가능성을 보여주었다는 점에서 매우 의미 있는 연구 결과라고 생각한다. 본 연구에서 제시하는 새로운 치료전략이 알츠하이머병 치료에 크게 기여할 수 있기를 기대하며, 또 더 나아가 다양한 퇴행성 뇌질환 치료에 확대 적용할 수 있을 것이라 생각한다.

---

핵심되는 말: 알츠하이머병, 집속초음파, 뇌혈관장벽, 베타아밀로이드, 아두카누맵

## PUBLICATION LIST

1. Shin J, **Kong C**, Lee J, Choi BY, Sim J, Koh CS, Park M, Na YC, Suh SW, Chang WS, Chang JW. Focused ultrasound-induced blood-brain barrier opening improves adult hippocampal neurogenesis and cognitive function in a cholinergic degeneration dementia rat model. *Alzheimer's research & therapy* 2019;11:1-15.
2. Shin J, **Kong C**, Cho JS, Lee J, Koh CS, Yoon MS, Na YC, Chang WS, Chang JW. Focused ultrasound-mediated noninvasive blood-brain barrier modulation: Preclinical examination of efficacy and safety in various sonication parameters. *Neurosurgical focus* 2018;44:E15.
3. Lee J, Chang WS, Shin J, Seo Y, **Kong C**, Song BW, Na YC, Kim BS, Chang JW. Non-invasively enhanced intracranial transplantation of mesenchymal stem cells using focused ultrasound mediated by overexpression of cell-adhesion molecules. *Stem cell research* 2020;43:101726.
4. **Kong C**, Park SH, Shin J, Beak HG, Park J, Na YC, Chang WS, Chang JW Factors associated with energy efficiency of focused ultrasound through the skull: A study of 3D-printed skull phantoms and its comparison with clinical experiences. *Frontiers in Bioengineering and Bio technology*. 2021;9:783048

5. Kim J, Shin J, **Kong C**, Lee S-H, Chang WS, Han SH. The synergistic effect of focused ultrasound and biophotonics to overcome the barrier of light transmittance in biological tissue. *Photodiagnosis and Photodynamic Therapy* 2021;33:102173.